Seismic analysis of nonlinear reinforced concrete frame structures

José Vittor S. Cóco[1], Mauro Schulz[1]

[1]*Dept. of Civil Engineering, Federal Fluminense University*
Rua Passo da Pátria 156, Bloco D, Niterói, RJ 24210-240, Brazil
josevittor@id.uff.br, mschulz@id.uff.br

Abstract. The behavior of structures subjected to ground motion must be thoroughly understood to mitigate risks and ensure compliance with safety standards The internal forces provided by the Response Spectrum Method, in the frequency domain, are not always suitable for the design of reinforced concrete structures. The behavior of concrete is different under compression and tension. The sum of the modal absolute values through SRSS (Square Root of the Sum of Squares) and CQC (Complete Quadratic Combinations) approaches provides maximum absolute internal forces. However, negative or positive values indicate compression and tension, and reinforcement design is greatly influenced by whether stresses are compressive or tensile. The purpose of this research is to present a methodology for the seismic dynamic analysis of nonlinear framed structures, in the time domain, in which the equilibrium is rigorously examined at the end of each time step. Constitutive models adopted for the cyclic behavior of concrete and steel are discussed. A Timoshenko beam element suitable for this nonlinear analysis is presented. The time integration algorithm is based on Newmark's implicit method. Equilibrium conditions are guaranteed at the end of each time step through an iterative process. The damping matrix uses the classic Rayleigh formulation. Equivalent nodal forces are calculated from accelerograms. An example is presented and conclusions are drawn. Comparison with experimental data shows that the model acceptably predicts the dynamic response of such structure for design purposes.

Keywords: seismic analysis, nonlinear structures, reinforced concrete.

1 Introduction

Seismic structural analysis attracts significant interest since careful analysis of the dynamic response of structures is necessary to ensure their safety. In particular, certain critical infrastructures, such as nuclear power plants, demand rigorous seismic analysis.

One common approach in this dynamic analysis is the Response Spectrum Method (RSM), which operates in the frequency domain. The RSM involves summing the modal absolute values through Square Root of the Sum of the Squares and Complete Quadratic Combination methods. However, these methods do not always provide accurate estimates of the maximum forces in the rebars of nonlinear structures. Whether forces are negative or positive relative to the global coordinate system is crucial information for structural design, as these indicate whether stress is compressive or tensile, respectively.

This work aims to apply a methodology for the dynamic seismic analysis of nonlinear frame structures in the time domain. A finite element method based on Timoshenko beam theory is selected to model three-dimensional reinforced concrete frame structures. The physical nonlinearity of materials is considered for normal stresses, while shear stresses are linearly estimated. Material constitutive relations from the literature are used to ensure reliability in stress-strain analysis. Equivalent nodal forces are obtained from accelerograms. Time integration uses Newmark's implicit method. This model is applied to a structure tested by Clough and Gidwani [1] and later discussed by Filippou et al [2]. The results are compared and discussed.

2 Timoshenko beam element formulation

A Timoshenko beam finite element with four nodes and rectangular cross section is used in this study. A small displacement approach from the nonlinear formulation presented in Braz and Schulz [3] is used.

The displacements at a point X_1, X_2, X_3 are expressed by $u_1 = U_1\ X_1\ - \theta_3\ X_1\ X_2 + \theta_2\ X_1\ X_3$, $u_2 = U_2\ X_1\ - \theta_1\ X_1\ X_3$, and $u_3 = U_3\ X_1\ + \theta_1\ X_1\ X_2$. U_i and θ_i are respectively the displacements and the rotations of the cross section at direction X_i, where $i = 1, 2, 3$. The normal strain is defined as $\varepsilon_{11}\ X_1\ = U_1' - \theta_3' X_2 + \theta_2' X_3$. Shear strains in X_2 and X_3 directions are $\gamma_{12}\ X_1\ = \phi_2 - \theta_1' X_3$ and $\gamma_{13}\ X_1\ = \phi_3 + \theta_1' X_2$, respectively. Shear distortions are given by $\phi_2 = -\theta_3 + U_2'$ and $\phi_3 = \theta_2 + U_3'$. The notation $' = \partial \big/ \partial X_1$ is used for simplicity.

The principle of minimum strain-energy yields

$$\int_V \delta\varepsilon_{11}\sigma_{11} dV = \delta\mathbf{u}^T \mathbf{f}_n \quad ; \quad \int_V \delta\gamma_{12}\sigma_{12} + \delta\gamma_{13}\sigma_{13}\ dV = \delta\mathbf{u}^T \mathbf{f}_s \tag{1}$$

where V is the volume and $\mathbf{u}$ is the displacement vector of the beam element. Normal stresses are denoted as σ_{11}, and shear stresses in X_2 and X_3 directions are σ_{12} and σ_{13}, respectively. The nodal force vector is given by $\mathbf{f} = \mathbf{f}_n + \mathbf{f}_s$, where $\mathbf{f}_n$ and $\mathbf{f}_s$ respectively denote the normal and shear force components.

The hypothesis that plane cross sections remain plane but not necessarily normal to the deformed axis yields the nodal normal strain component, i.e.

$$\varepsilon_{11}\ X_1\ = \mathbf{x}^T \boldsymbol{\varepsilon}_n\ X_1\ \quad ; \quad \boldsymbol{\varepsilon}_n\ X_1\ = \begin{bmatrix} U_1' & -\theta_3' & \theta_2' \end{bmatrix}^T \quad ; \quad \boldsymbol{\varepsilon}_n\ X_1\ = \mathbf{B}_n^T\ X_1\ \mathbf{u} \tag{2}$$

where $\mathbf{x} = \begin{bmatrix} 1 & X_2 & X_3 \end{bmatrix}^T$ is the position vector and $\mathbf{B}_n$ is the Lagrange interpolation matrix for normal strains.

The substitution of eq. (2) in the normal component of eq. (1) results in

$$\int_L \mathbf{B}_n\, \mathbf{s}_n\, dX_1 = \mathbf{f}_n \tag{3}$$

where L is the beam length and vector $\mathbf{s}_n = \begin{bmatrix} N_1 & M_2 & M_3 \end{bmatrix}^T$ corresponds to the normal internal forces.

The shear component of eq. (1) may be rewritten according to the definitions of γ_{12} and γ_{13}, which yields

$$\int_L \delta\phi_2 V_2 + \delta\phi_3 V_3 + \delta\theta_1' T_1\ dX_1 = \int_L \delta\boldsymbol{\varepsilon}_s^T\, \mathbf{s}_s\ dX_1 = \delta\mathbf{u}^T \mathbf{f}_s \tag{4}$$

where $\mathbf{s}_s\ X_1\ = \begin{bmatrix} V_2 & V_3 & T_1 \end{bmatrix}^T$ is the shear internal forces. Vector $\boldsymbol{\varepsilon}_s\ X_1\ = \begin{bmatrix} \phi_2 & \phi_3 & \theta_1' \end{bmatrix}^T$ is determined by $\boldsymbol{\varepsilon}_s\ X_1\ = \mathbf{B}_s^T\ X_1\ \mathbf{u}$, such that $\mathbf{B}_s$ is the Lagrange interpolation matrix for shear strains. Equation (4) yields

$$\int_L \mathbf{B}_s\, \mathbf{s}_s\, dX_1 = \mathbf{f}_s \tag{5}$$

The equation of equilibrium is obtained from eqs. (3) and (5), i.e.

$$\int_L \mathbf{B}_n\, \mathbf{s}_n\, dX_1 + \int_L \mathbf{B}_s\, \mathbf{s}_s\, dX_1 = \mathbf{f} \tag{6}$$

The linearized incremental equation is expressed by

$$\int_L \mathbf{B}_n \Delta\mathbf{s}_n\, dX_1 + \int_L \mathbf{B}_s\, \Delta\mathbf{s}_s\, dX_1 = \Delta\mathbf{f} \tag{7}$$

Incremental normal stresses and strains are related by $\Delta\sigma_{11} = E\,\Delta\varepsilon_{11}$, where E is the derivative of the nonlinear constitutive equation $\sigma_{11}\ \varepsilon_{11}$. From eq. (2), $\Delta\sigma_{11}$ is defined by

$$\Delta\mathbf{s}_n = \mathbf{D}_n \Delta\boldsymbol{\varepsilon}_n = \mathbf{D}_n \mathbf{B}_n^T\, \Delta\mathbf{u} \quad ; \quad \mathbf{D}_n = \int_A \mathbf{x}\, E\, \mathbf{x}^T dA \tag{8}$$

A linear elastic incremental shear stresses and strains relation, i.e. $\mathbf{s}_s = \mathbf{D}_s\, \boldsymbol{\varepsilon}_s$, yields

$$\Delta\mathbf{s}_s = \mathbf{D}_s\, \Delta\boldsymbol{\varepsilon}_s = \mathbf{D}_s\, \mathbf{B}_s^T\, \Delta\mathbf{u} \tag{9}$$

The diagonal 3×3 matrix $\mathbf{D}_s$ is defined by its elements $D_{s11} = D_{s22} = k_s GA$ and $D_{s33} = GJ$, where G and J are the shear modulus and the torsional stiffness, respectively. The shear coefficient is taken as

$k_s = 10\ (1+\nu) \,/\, (12+11\nu)$, as suggestion by Cowper [4].

The substitution of eqs. (8) and (9) in eq. (7) yields the tangent stiffness matrix $\mathbf{K}$, which is given by

$$\mathbf{K}\,\Delta\mathbf{u} = \Delta\mathbf{f} \quad ; \quad \mathbf{K} = \int_L \mathbf{B}_n\,\mathbf{D}_n\,\mathbf{B}_n{}^T + \mathbf{B}_s\,\mathbf{D}_s\,\mathbf{B}_s{}^T \; dX_1 \tag{10}$$

Integrals in eqs. (6) and (10) are numerically resolved by Gauss-Legendre quadrature and reduced integration. Three integration points are used in a four-node beam element.

3 Concrete constitutive model

Concrete fiber discretization must adequately account for confined and unconfined concrete fibers. Confined and unconfined concrete zones are bounded by the outer face of the stirrup-tie. The strength increase factor due to confinement is defined as $K_c = 1 + \rho_s f_{yh} / f_c$, where ρ_s is the ratio between the volume of the hoop set and the volume of concrete core, f_c is the concrete compressive strength, and f_{yh} is the yield strength of stirrups or hoop sets. For unconfined concrete, $K_c = 1$.

The compressive monotonic curve by Kent and Park [5], as modified by Scott et al. [6], is adopted (Fig. 1). Tensile stresses are neglected. For concrete strains greater than $\varepsilon_{c0} = -0.002K_c$, the Hognestad parabola is considered. Otherwise, the monotonic curve follows a line segment with softening slope Z , which is given by

$$Z = 0.5 / \left[\, 3 + 0.29 f_c \,/\, (145 f_c - 1000) + 0.75\rho_s \sqrt{h_{core}/s_h} \,\right] - 0.002K_c \tag{11}$$

where h_{core} is the height of the confined concrete zone, and s_h is the spacing between stirrups per unit length. Concrete stress remains steady if minimum compressive stress $\sigma_{cmin} = -0.2K_c f$ is reached. The ultimate compressive strain is taken as $\varepsilon_{cu} = -0.004 - 0.9\rho_s \left(f_{yh} / 300\,\text{MPa} \right)$. For unconfined concrete, $\varepsilon_{cu} = -0.004$.

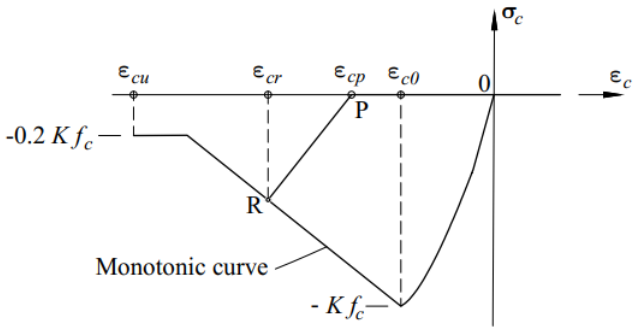

Figure 1. Concrete constitutive stress-strain model

In the case of unloading, an unloading curve is established by the line connecting points R and P (Fig 1). The strain ε_{cr} at point R is the strain at reversal. The strain ε_{cp} at point P is defined by Karsan and Jirsa [7] as

$$\varepsilon_{cp}/\varepsilon_{c0} = \begin{cases} 0.145\,(\varepsilon_{cr}/\varepsilon_{c0})^2 + 0.127\,(\varepsilon_{cr}/\varepsilon_{c0}) & \text{se} \quad \varepsilon_{cr}/\varepsilon_{c0} < 2 \\ 0.707\,(\varepsilon_{cr}/\varepsilon_{c0} - 2) + 0.834 & \text{se} \quad \varepsilon_{cr}/\varepsilon_{c0} \geq 2 \end{cases} \tag{12}$$

Concrete stress is zero for strains greater than ε_{cp} . In the case of further reloading and unloading, the unloading path is followed until concrete strain is smaller than ε_{cr} , when it returns to the original monotonic curve. Further unloading paths may be established by eq. (12) if unloading starts on the monotonic curve.

4 Steel constitutive model

This study follows the steel model by Menegotto and Pinto [8], as modified by Filippou et al. [9].

Yield stress and strain are denoted by σ_{sy} and ε_{sy} , respectively, such that $\sigma_{sy} = f_y$, where f_y is the yield

strength of steel. The monotonic envelope curve follows the line segment with slope equal to the steel initial modulus E_{s0}. After yielding, the plastic slope is considered as $E_{s1} = b\,E_{s0}$, where b is a material parameter.

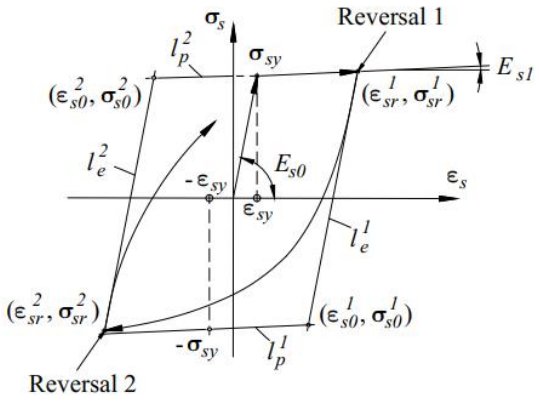

Figure 2. Steel constitutive stress-strain model

The stress-strain trajectory of steel stress σ_s and strain ε_s remains within the monotonic curve until unloading happens on the plastic line. The reversal curve (Fig. 2) is defined by Menegotto and Pinto [8] in terms of the normalized stress σ_s^* and strain ε_s^*, i.e.

$$\sigma_s^* = b\,\varepsilon_s^* + \left(1-b\right)\varepsilon_s^* \Big/ \left(1+\varepsilon_s^{*R}\right)^{1/R} \tag{13}$$

$$\sigma_s^* = \left(\sigma_s - \sigma_{sr}\right) \Big/ \left(\sigma_{s0} - \sigma_{sr}\right) \tag{14}$$

$$\varepsilon_s^* = \left(\varepsilon_s - \varepsilon_{sr}\right) \Big/ \left(\varepsilon_{s0} - \varepsilon_{sr}\right) \tag{15}$$

where σ_{sr} and ε_{sr} are the stress and strain at reversal, respectively, while σ_{s0} and ε_{s0} are the stress and strain at the intersection between lines l_e and l_p. R is a curvature parameter which accounts for the whole loading history. The modified model by Filippou et al. [9] allows R to be determined solely in respect to the previous reversal trajectory. The steel isotropic strain hardening effect is also implemented in this later model.

The tangent constitutive relation $\partial\sigma_s/\partial\varepsilon_s$ considers the chain rule of derivatives, i.e.

$$\partial\sigma_s/\partial\varepsilon_s = \left(\partial\sigma_s/\partial\varepsilon_s^*\right)\left(\partial\varepsilon_s^*/\partial\varepsilon_s\right) \tag{16}$$

5 Time integration method

The equation of motion of a structure with nonlinear behavior is

$$\mathbf{M}\ddot{\mathbf{u}} + \mathbf{C}\dot{\mathbf{u}} + \mathbf{f}\left(\mathbf{u}\right) = \mathbf{p} \tag{17}$$

where $\mathbf{M}$ is the mass matrix, $\mathbf{C}$ is the damping matrix, and $\mathbf{f}$ is the restoring force vector, as defined by eq. (6). $\mathbf{u}\left(t\right)$ is the displacement vector and $\mathbf{p}\left(t\right)$ is the external force vector, where t denotes time. The velocity and acceleration vectors are $\dot{\mathbf{u}} = d\mathbf{u}/dt$ and $\ddot{\mathbf{u}} = d^2\mathbf{u}/dt^2$, respectively.

In time-step $i+1$, $\mathbf{u}_{i+1}$ is initially approximated as $\mathbf{u}_i$. Implicit acceleration $\ddot{\mathbf{u}}_{i+1}$ and velocity $\dot{\mathbf{u}}_{i+1}$ are

$$\ddot{\mathbf{u}}_{i+1}\left(\mathbf{u}_{i+1}\right) = \frac{1}{\Delta t^{\,2}\,\beta}\left(\mathbf{u}_{i+1} - \mathbf{u}_i\right) - \frac{1}{\Delta t\;\beta}\dot{\mathbf{u}}_i - \left(\frac{1}{2\beta} - 1\right)\ddot{\mathbf{u}}_i \tag{18}$$

$$\dot{\mathbf{u}}_{i+1}\left(\mathbf{u}_{i+1}\right) = \frac{\gamma}{\Delta t\;\beta}\left(\mathbf{u}_{i+1} - \mathbf{u}_i\right) + \left(1 - \frac{\gamma}{\beta}\right)\dot{\mathbf{u}}_i + \Delta t\left(1 - \frac{\gamma}{2\beta}\right)\ddot{\mathbf{u}}_i \tag{19}$$

where $\gamma = 1/2$ and $\beta = 1/4$ are integration constants for stability and convergence.

The residual function $\mathbf{g}$ ensures that eq. (17) is satisfied, i.e.

$$\mathbf{g}\ \mathbf{u}_{i+1}\ = \mathbf{M}\ddot{\mathbf{u}}_{i+1} + \mathbf{C}\dot{\mathbf{u}}_{i+1} + \mathbf{f}\ \mathbf{u}_{i+1}\ - \mathbf{p}_{i+1} = 0 \tag{20}$$

The displacement vector $\mathbf{u}_{i+1}^{\langle j \rangle}$ at iteration j should meet the criteria $\left\| \mathbf{g}\ \mathbf{u}_{i+1}^{\langle j \rangle} \right\| \leq \text{tol}$. If the former expression is not respected, $\mathbf{u}_{i+1}^{\langle j+1 \rangle}$ at iteration $j+1$ is obtained by

$$\mathbf{K}_{eff}\ \Delta\mathbf{u}_{i+1} = -\mathbf{g}\ \mathbf{u}_{i+1}^{\langle j \rangle} \tag{21}$$

$$\mathbf{K}_{eff} = \frac{\partial \mathbf{g}\ \mathbf{u}_{i+1}^{\langle j \rangle}}{\partial \mathbf{u}_{i+1}} = \mathbf{M}\frac{1}{\Delta t^{\ 2}\ \beta} + \mathbf{C}\ \mathbf{u}_{i+1}\ \ \frac{\gamma}{\Delta t\ \ \beta} + \mathbf{K}\ \mathbf{u}_{i+1}^{\langle j \rangle} \tag{22}$$

$$\mathbf{u}_{i+1}^{\langle j+1 \rangle} = \mathbf{u}_{i+1}^{\langle j \rangle} + \Delta\mathbf{u}_{i+1} \tag{23}$$

where the tangent stiffness matrix $\mathbf{K}$ is obtained from eq. (10).

The damping matrix $\mathbf{C}\ \mathbf{u}_{i+1}$ is considered as Rayleigh classic damping, which is approximately given as proportional to the mass and stiffness matrices, i.e.

$$\mathbf{C} = c_1\,\mathbf{M} + c_2\,\mathbf{K}\ \mathbf{u}_{i+1}^{\langle 0 \rangle} \tag{24}$$

where c_1 and c_2 are constants. $\mathbf{C}$ is determined at the beginning of each time-step and is not updated along the iterative procedure, as suggested by Filippou et al. [2].

Considering that the damping ratio value is constant for all natural modes of vibration yields $c_1 = 2\zeta\,\omega_1\,\omega_2 / \ \omega_1 + \omega_2$ and $c_2 = 2\zeta / \ \omega_1 + \omega_2$, where ζ is the damping ratio. ω_1 and ω_2 are respectively the angular natural frequencies of the first and second natural modes of vibration of the associated undamped system.

6 Equivalent earthquake nodal forces

This item discusses two nonlinear seismic analysis models. The actual model assumes that earthquake forces are applied at foundation nodes, which are subjected to rigid body movements. The analytical model restricts the foundation nodes and apply equivalent forces to the remaining nodes of the structure, which are considered free.

The equation of motion of the actual model is expressed by

$$\begin{bmatrix} \mathbf{M}_{FF} & \mathbf{0} \\ \mathbf{0} & \mathbf{M}_{RR} \end{bmatrix} \begin{bmatrix} \ddot{\mathbf{u}}_L \\ \ddot{\mathbf{u}}_R \end{bmatrix} + \begin{bmatrix} \mathbf{f}_F\ \mathbf{u} \\ \mathbf{f}_R\ \mathbf{u} \end{bmatrix} = \begin{bmatrix} \mathbf{0} \\ \mathbf{p}_R\ \ t \end{bmatrix} \tag{25}$$

where subscripts R and F stand for the foundation and remaining nodes of the structure, which are respectively restrained and free in the analytical model. The displacement vector is $\mathbf{u} = \begin{bmatrix} \mathbf{u}_L & \mathbf{u}_R \end{bmatrix}^T$. Mass $\mathbf{M}$ is simplified as a diagonal matrix. Damping $\mathbf{C}$ is neglected. External force vector $\mathbf{p}_R\ \ t$ represents the earthquake loads, which are applied at foundation level in the actual model. Force vector $\mathbf{f} = \begin{bmatrix} \mathbf{f}_L & \mathbf{f}_R \end{bmatrix}^T$ is determined by eq. (6).

The equation of motion of the analytical model is expressed by removing from eq. (25) the rigid body movement at foundation level, which is represented by $\begin{bmatrix} \bar{\mathbf{u}}_L & \mathbf{u}_R \end{bmatrix}$, and by considering that $\mathbf{f}$ does not change.

$$\begin{bmatrix} \mathbf{M}_{LL} & \mathbf{0} \\ \mathbf{0} & \mathbf{M}_{RR} \end{bmatrix} \begin{bmatrix} \ddot{\mathbf{u}}_L - \ddot{\bar{\mathbf{u}}}_L \\ \ddot{\mathbf{u}}_R - \ddot{\mathbf{u}}_R \end{bmatrix} + \begin{bmatrix} \mathbf{f}_F\ \mathbf{u} \\ \mathbf{f}_R\ \mathbf{u} \end{bmatrix} = \begin{bmatrix} \mathbf{p}_L^*\ \ t \\ \mathbf{p}_R^*\ \ t \end{bmatrix} \tag{26}$$

Subtracting eq. (25) from eq. (26) yields the dynamic-equivalent applied forces at free nodes in the analytical model and its reactions at restrained nodes, which are, respectively, $\mathbf{p}_L^*\ \ t\ = -\mathbf{M}_{LL}\ddot{\bar{\mathbf{u}}}_L$ e $\mathbf{p}_R^*\ \ t\ = \mathbf{p}_R\ \ t$.

7 Example

The test conducted by Clough and Gidwani [1] investigates the behavior of a two-story building subjected to an earthquake in the main horizontal direction. Concrete blocks were added to increase vibration response. In this study, the structure was modeled as a two-story frame, considering its geometric symmetry in the y direction (Fig. 3). Weight and mass from the half concrete blocks, as well as from the half-transverse beams, are distributed over their respective supporting nodes. Material properties are adopted according to data presented by the test authors. Due to a lack of data on the b parameter of steel, the values suggested by Filippou et al [2] are used.

Since the proposed beam element is limited to rectangular sections, elements in zone 1, defined in Fig. 3, are considered elastic, such that their cross-sectional areas and moments of inertia, including slab contribution, are adopted for the cracked section according to the values suggested by Filippou et al [2]. Elements in zone 2, where a greater effect of material plasticity is expected, are assumed to be nonlinear and have a rectangular cross section.

The earthquake was simulated on a shaking table following the N69W accelerogram of the Kern County Earthquake, measured by the Taft Lincoln Tunnel station, California, 1952. Ground motion was tested in three stages, scaled at peak accelerations of 0.095g, 0.57g, and 0.65g. In this study, only the 0.57g stage was analyzed. Figure 4 shows the scaled accelerogram, as retrieved from the Center of Engineering Strong Motion [10] database.

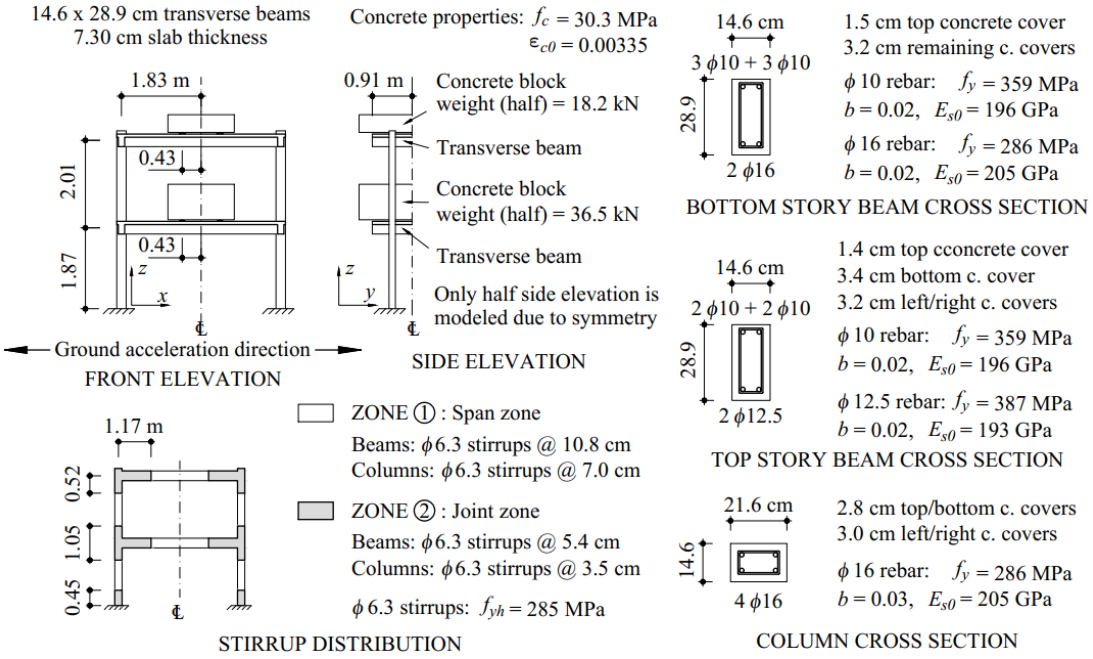

Figure 3. Two-story building model

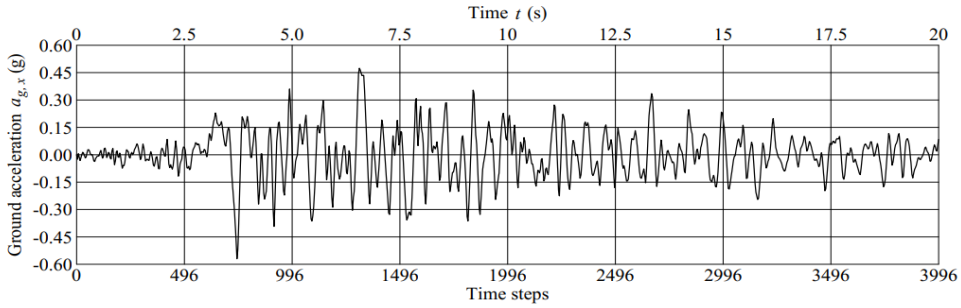

Figure 4. Taft 1952 N69W accelerogram

The displacement histories on each floor, as obtained by the analytical model, are presented in Fig. 5. The analytical results agrees with the experimental maximum and minimum displacements at the top and bottom stories

($\delta_{x\max}^{TOP}$ = 0.057, $\delta_{x\min}^{TOP}$ = -0.070, $\delta_{x\max}^{BOTTOM}$ = 0.038, and $\delta_{x\min}^{BOTTOM}$ = -0.050 m).

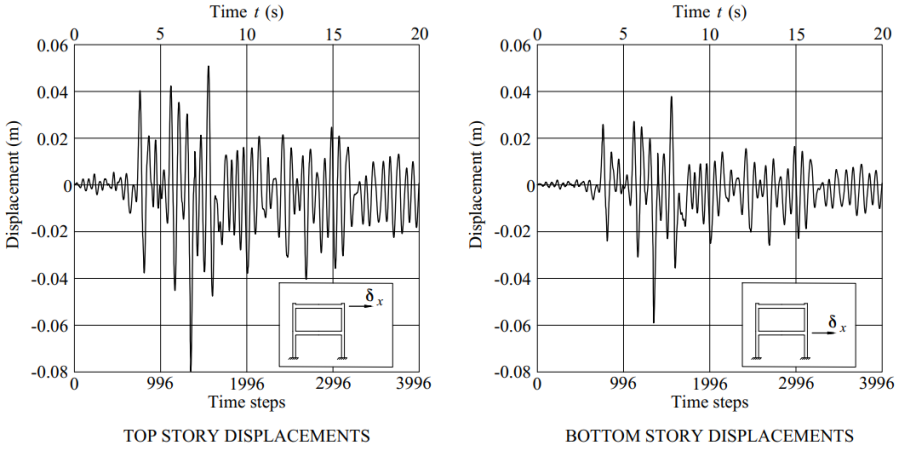

Figure 5. Displacement history results from the analytical model

8 Conclusions

When compared to the test results as presented in Clough and Gidwani [1], the maximum and minimum displacements of the analytical model are close to those of the test, favoring safety for design purposes. Remaining displacements are relatively smaller after peak accelerations, i.e. after 7.5 s. This is mostly due to the effects of bond deterioration and slippage of rebars, which are not considered in the element formulation. Filippou et al [2] discuss the influence of reinforcement slippage on dynamic response, justifying the observed difference. The study of bond effects is an object for further developments.

Acknowledgements. The first author thanks the Coordenação de Aperfeiçoamento de Pessoal de Nível Superior (CAPES) for the financial support.

Authorship statement. The authors hereby confirm that they are the sole liable persons responsible for the authorship of this work, and that all material that has been herein included as part of the present paper is either the property (and authorship) of the authors, or has the permission of the owners to be included here.

References

[1] R.W. Clough and J. Gidwani, "Reinforced Concrete Frame 2: Testing and Analytical Correlation", Report No. EERC 76-15, Earthquake Engineering Research Center, University of California, Berkeley, 1976.
[2] F. C. Filippou, A. D'Ambrisi and A. Issa, "Nonlinear Static and Dynamic Analysis of Reinforced Concrete Subassemblages", Rep. No. UCB/EERC–92/08, Earthquake Engineering Research Center, Un. of California, Berkeley, 1992.
[3] L. F. C. R. Braz and M. Schulz, " Estabilidade de estruturas tubulares em situação de içamento", Revista da Estrutura de Aço - REA, vol. 10, n. 3, pp. 312–332, 2021.
[4] G. R. Cowper, “The shear coefficient in Timoshenko’s beam theory”, J. of Applied Mechanics, v. 33, pp. 335-340, 1966.
[5] D. C. Kent and R. Park, “Flexural Members with Confined Concrete”, J. Str. Division, ASCE, 97(ST7), 1971.
[6] B. D. Scott, R. Park and M. J. N. Priestley, “Stress-Strain Behavior of Concrete Confined by Overlapping Hoops at Low and High Strain Rates”, ACI Journal, v. 79, n. 1, pp. 13-27, 1982.
[7] L. D. Karsan, J. O. Jirsa, “Behavior of Concrete under Compressive Loadings”, J. Str. Division, ASCE, 95(ST12), 1969.
[8] M. Menegotto and P. E. Pinto, “Method of analysis for cyclically loaded R.C. plane frames including changes in geometry and non-elastic behaviour of elements under combined normal force and bending”, In Preliminary Report 13, IABSE, pp. 15–22, Lisbon, 1973.
[9] F. C. Filippou, E P. Popov and V V. Bertero, “Effects of Bond Deterioration on Hysteretic Behavior of Reinforced Concrete Joints”, EERC Report 83-19, Earthquake Engineering Research Center, Berkeley, 1983.
[10] Center of Engineering Strong Motion, accessed 7 June 2024, <https://www.strongmotioncenter.org/cgi-bin/CESMD/archive.pl>.